Laser and Particle Beams (2004), *22*, 69–74. Printed in the USA.

DOI: 10.1017/S0263034604221139

Solutions of the nonlinear paraxial equation due to laser plasma–interactions

F. OSMAN,[1] R. BEECH,[1] AND H. HORA[2]

[1]School of Quantitative Methods & Mathematical Sciences, University of Western Sydney, Penrith South, Australia
[2]Department of Theoretical Physics, University of New South Wales, Sydney, Australia

(RECEIVED 28 May 2003; ACCEPTED 17 November 2003)

Abstract

This article presents a numerical and theoretical study of the generation and propagation of oscillation in the semiclassical limit $\hbar \to 0$ of the nonlinear paraxial equation. In a general setting of both dimension and nonlinearity, the essential differences between the "defocusing" and "focusing" cases are observed. Numerical comparisons of the oscillations are made between the linear ("free") and the cubic (defocusing and focusing) cases in one dimension. The integrability of the one-dimensional cubic nonlinear paraxial equation is exploited to give a complete global characterization of the weak limits of the oscillations in the defocusing case.

Keywords: Laser-plasma interactions; Nonlinear paraxial equation; Oscillations; Wave propagation

1. INTRODUCTION

Wave propagation in plasmas with substantial dispersion or diffraction and a significant nonlinearity can be described by the nonlinear paraxial equation for laser plasma interaction. The nonlinear paraxial equation has exact soliton solutions (Häuser *et al*., 1992) that correspond to a balance between nonlinearity and dispersion in the case of temporal solitons or between nonlinearity and diffraction in the case of spatial solitons. The soliton concept is a sophisticated mathematical construct based on the integrability of a class of nonlinear differential equations. Integrable nonlinear differential equations have one feature in common; they are all conservative if dissipation is neglected (Hora, 1991, Chapter 10.6), thus derivable from a Hamiltonian. The integration is performed via the method of inverse scattering (Zakharov & Shabat, 1973).

A numerical study of the semiclassical limit of linear and nonlinear paraxial equations, in both focusing and defocusing cases, is explored. Along with this, an analytical study of the semiclassical limit of the defocusing cases will also be investigated. Comparisons of both dimension and nonlinearity are observed for the focusing and defocusing cases, respectively, due to laser–plasma interactions (Osman, 1998). This work is of interest to the acceleration of electrons by lasers (Esarey *et al*., 1997; Wang *et al*, 1998; Hora, 2000) and for the scheme of the fast ignitor for laser-driven inertial confinement fusion (Tabak *et al*, 1993; Hora, 2000).

Address correspondence and reprint requests to: F. Osman, School of Quantitative Methods and Mathematical Sciences, University of Western Sydney, Locked Bag 1797, Penrith South DC NSW 1797, Australia. E-mail: f.osman@uws.edu.au

2. NONLINEAR PARAXIAL EQUATION

One of the simplest nonlinear equations is the nonlinear paraxial equation for a complex valued field $\Psi(x, t)$ over a spatial domain $\Omega \subset R^D$ (Osman, 1998):

$$i\hbar\partial_t \Psi + \frac{\hbar^2}{2}\Delta\Psi - U'(|\Psi|^2)\Psi = 0, \tag{1}$$

where U' is the first derivative of a twice-differentiable nonlinear real-valued function and $\hbar$ is a positive parameter. The parameter $\hbar$ is analogous to Planck's constant, which in the quantum setting is usually very small when evaluated in the natural dimensional scales of the equation as determined by its initial and boundary conditions. For the moment, the precise specification of the domain Ω and the nature of the boundary conditions are left vague in order to make some general statements regarding the structure of Eq. (1). The nonlinear function $U : R_+ \to R$ is the potential energy density of the field and is clearly seen when the nonlinear par-

axial equation, Eq. (1), is recast as a Hamiltonian system in the form

$$i\hbar\partial_t\Psi = \frac{\partial H}{\partial\bar{\Psi}}, \quad H = \int_\Omega \frac{\hbar^2}{2}|\nabla\Psi|^2 + U(|\Psi|^2)\,d^Dx. \tag{2}$$

The associated Poisson bracket of any two functionals F and G is given by

$$\{F,G\} \equiv \frac{1}{i\hbar}\int_\Omega\left(\frac{\partial F}{\partial\Psi}\frac{\partial G}{\partial\bar{\Psi}} - \frac{\partial F}{\partial\bar{\Psi}}\frac{\partial G}{\partial\Psi}\right)d^Dx. \tag{3}$$

The evolution of any functional F under the nonlinear paraxial equation flow (1) is then

$$\frac{dF}{dt} = \{F,H\}. \tag{4}$$

This Hamiltonian structure plays a major role in our analysis. Associated with the nonlinear paraxial equation, (1), are the local conservation laws corresponding to mass, momentum, and energy conservation. Their densities ρ, μ, and ε, respectively, are given by

$$\rho = |\Psi|^2,$$

$$\mu = -i\frac{\hbar}{2}(\bar{\Psi}\nabla\Psi - \Psi\nabla\bar{\Psi})$$

$$\varepsilon = \frac{\hbar^2}{2}|\nabla\Psi|^2 + U(|\Psi|^2). \tag{5}$$

The mass and momentum densities determine the field φ up to a constant phase; the energy density can be written in terms of them as

$$\varepsilon = \frac{1}{2}\frac{|\mu|^2}{\rho} + \frac{\hbar^2}{8}\frac{|\nabla\rho|^2}{\rho} + U(\rho). \tag{6}$$

The local conservative laws are then

$$\partial_t\rho + \nabla\cdot\mu = 0,$$

$$\partial_t\mu + \nabla\cdot\left(\frac{\mu\otimes\mu}{\rho}\right) + \nabla P(\rho) = \frac{\hbar^2}{4}\nabla\cdot[\rho\nabla^2\log\rho]$$

$$\partial_t\varepsilon + \nabla\cdot\left(\frac{\mu}{\rho}(\varepsilon + P(\rho))\right) = \frac{\hbar^2}{4}\nabla\cdot\left[\frac{\mu\Delta\rho}{\rho} - \frac{\nabla\cdot\mu\nabla\rho}{\rho}\right], \tag{7}$$

where $P(\rho) \equiv \rho U'(\rho) - U(\rho)$.

The first two of these are a closed system govering ρ and μ that has the form of a perturbation of the compressible Euler equations of fluid dynamics with the "pressure" given by $P(\rho)$. If the "Euler part" of these equations is to be hyperbolic, then the "pressure" $P(\rho)$ must be a strictly increasing function of ρ; in that case $P'(\rho) = \rho U''(\rho) > 0$. This means that U must be a strictly convex function of ρ and corresponds to a "defocusing" nonlinear paraxial equation. In this context a "focusing" nonlinear paraxial equation can be understood as a fluid whose pressure decreases when the mass density increases, a phenomenon leading to the development of mass concentrations.

3. THE SEMICLASSICAL LIMIT

The "semiclassical limit" of the nonlinear paraxial equation can be described as follows. Consider the family, parameterized by $\hbar > 0$, of solutions $\Psi^{(\hbar)}(x,t)$ to the Cauchy problems (Osman, 1998):

$$i\hbar\partial_t\Psi^{(\hbar)} + \frac{\hbar^2}{2}\Delta\Psi^{(\hbar)} - U'(|\Psi^{(\hbar)}|^2)\Psi^{(\hbar)} = 0 \tag{8a}$$

$$\Psi^{(\hbar)}(x,0) = A(x)\exp\left(\frac{i}{\hbar}S(x)\right), \tag{8b}$$

where the (nonnegative) amplitude $A(x)$ and (real) phase $S(x)$ are assumed to be smooth and independent of $\hbar$. The initial conserved densities are then

$$\rho^{(\hbar)}(x,0) = |A(x)|^2$$

$$\mu^{(\hbar)}(x,0) = |A(x)|^2\nabla S(x) \tag{9a}$$

$$\varepsilon^{(\hbar)}(x,0) = \frac{1}{2}|A(x)|^2|\nabla S(x)|^2 + \frac{\hbar^2}{2}|\nabla A(x)|^2 + U(|A(x)|^2) \tag{9b}$$

The general problem of the semiclassical limit is to determine the limiting behavior of any function of the field $\Psi^{(\hbar)}$ as $\hbar\to 0$, in particular, to ascertain the existence (in some sense) of the limits of the conserved densities:

$$\rho = \lim_{h\to 0}\rho^{(\hbar)} \tag{10a}$$

$$\mu = \lim_{h\to 0}\mu^{(\hbar)} \tag{10b}$$

$$\varepsilon = \lim_{h\to 0}\varepsilon^{(\hbar)}, \tag{10c}$$

and if the limits exist, to determine their dynamics.

Arguing formally, it is natural to conjecture for the defocusing case that the $0(\hbar^2)$ dispersive terms appearing in Eq. (7) are negligible, as $\hbar\to 0$ and that the limiting densities ρ and μ satisfy the hyperbolic system (the Euler system)

$$\partial_t\rho + \nabla\cdot\mu = 0$$

$$\partial_t\mu + \nabla\cdot\left(\frac{\mu\otimes\mu}{\rho}\right) + \nabla P(\rho) = 0, \tag{11a}$$

with initial conditions inferred from Eq. (9a) given by

$$\rho(x,0) = |A(x)|^2, \qquad \mu(x,0) = |A(x)|^2\nabla S(x). \tag{11b}$$

https://doi.org/10.1017/S0263034604221139 Published online by Cambridge University Press

This argument is self-consistent only so long as the solution of the Euler system (11) remains classical. In that case, the limiting energy density will be given by

$$\varepsilon = \frac{1}{2}\frac{|\mu|^2}{\rho} + U(\rho), \tag{12}$$

and will satisfy

$$\partial_t \varepsilon + \nabla\cdot\left(\frac{\mu}{\rho}(\varepsilon + P(\rho))\right) = 0, \tag{13}$$

hence, playing the role of a Lax entropy for the Euler system (11). The genuinely nonlinear nature of the Euler system (11) will ensure that its classical solution will develop singular behavior (an infinite derivative) for all but rarefaction initial data. At the instant such a breaking occurs, the formally small dispersive terms on the right side of (11) will no longer be negligible, and the above characterization of the semiclassical limit will break down. Because this small regularizing term is dispersive, one expects that the impending singularity in ρ and μ will be regularized by the development of small wavelength oscillations.

4. THE NUMERICAL EXPERIMENTS ON THE ONSET OF BREAKING

Numerics are to be used to illustrate the breakdown of the "Euler" description of the semiclassical limit for the defocusing nonlinear paraxial equation (Fornberg & Whitham, 1978, p. 289). The problem is cast in one spatial dimension with a cubic nonlinearity (Osman, 1998):

$$i\hbar\partial_t \Psi = -\frac{\hbar^2}{2}\partial_{xx}\Psi + \gamma|\Psi|^2\Psi \tag{14a}$$

$$\Psi(x,0) = A_{in}(x)\exp\left(\frac{i}{\hbar}S_{in}(x)\right), \tag{14b}$$

where γ here is a positive constant. For this one-dimensional case, the Euler system in Eq. (11a), describing the formal semiclassical limit, reduces to the initial value problem:

$$\partial_t \rho + \partial_x \mu = 0$$

$$\partial_t \mu + \partial_x\left(\frac{\mu^2}{\rho} + \gamma\frac{\rho^2}{2}\right) = 0 \tag{15a}$$

$$\rho(x,0) = A_{in}^2(x), \qquad \mu(x,0) = A_{in}^2(x)\partial_x S_{in}(x). \tag{15b}$$

Riemann invariants for the Euler system (15a) are given by

$$r_\pm = \frac{\mu}{2\rho} \pm \sqrt{\gamma\rho}, \tag{16}$$

and the system can be placed in the Riemann invariant form

$$\partial_t r_+ - \frac{1}{2}(r_+ + 3r_-)\partial_x r_+ = 0$$

$$\partial_t r_- - \frac{1}{2}(3r_+ + r_-)\partial_x r_- = 0, \tag{17a}$$

with the initial conditions

$$r_\pm(x,0) = \frac{1}{2}\partial_x S_{in}(x) \pm \sqrt{\gamma}A_{in}(x). \tag{17b}$$

5. THE NUMERICAL EXPERIMENTS ON THE POSTBREAKING PHENOMENA

Another method for deriving the reduced system in Equation (15a) is the classical WKB method. It considers

$$i\hbar\partial_t \Psi^{(\hbar)} = -\frac{\hbar^2}{2}\partial_{xx}\Psi^{(\hbar)} + V(x)\Psi^{(\hbar)}, \tag{18}$$

and begins with the Ansatz that $\Psi^{(\hbar)}$ is in the form

$$\Psi^{(\hbar)}(x,t) = A(x,t)\exp\left(\frac{i}{\hbar}S(x,t)\right) + 0(\hbar). \tag{19}$$

Inserting this Ansatz into the nonlinear paraxial equation (18), and balancing the leading two powers of $\hbar$ yields

$$\partial_t u + u\partial_x u + \partial_x V = 0$$

$$\partial_t A + u\partial_x A + \frac{1}{2}A\partial_x u = 0, \tag{20}$$

where $u = \partial_x S$, which is equivalent to the reduced system in Eq. (15a) upon making the identifications

$$\rho = A^2, \qquad \mu = A^2 u. \tag{21}$$

The development of a singularity in this reduced system must then be interpreted as a breakdown in the Ansatz equation (19). After the breakdown, the time of the wave forms no longer continue to resemble that of the Ansatz.

In linear theories such as quantum mechanics and classical electromagnetism, the presence of singularities in reduced systems and their consequences for the full system are well understood. For example, in quantum mechanics the characteristics of the reduced hyperbolic system (20) are the paths of classical particles in the conservative force field $F(x) = -\partial_x V(x)$, which is defined in terms of the prescribed potential energy function $V(x)$. In this manner, classical mechanics arises as the semiclassical limit of quantum mechanics. (In the electromagnetic setting, the characteristics are the "rays" of "geometrical optics".)

Singularities in the reduced semiclassical equations result from foci and envelopes of families of these classical paths.

https://doi.org/10.1017/S0263034604221139 Published online by Cambridge University Press

These envelopes separate regions in the (x,t) plane that consist of points lying on only one classical path from regions consisting of points that lie on multiple paths. Along these envelopes (called caustics), neighboring rays coalesce and geometric conservation law properties of the transport equation for the amplitude $A(x,t)$ force $|A|$ to diverge along these caustics.

More mathematically, in the linear case of quantum mechanics, the reduced hyperbolic system is degenerate in the sense that the eikonal equation for k and the eikonal equation for A have identical characteristics. Because the eikonal equation does not depend upon the amplitude A, it can be solved first, and its characteristics are the classical paths. The transport equation for the amplitude A is then integrated along these classical paths, and geometrical consideration forces $|A|$ to diverge along caustic envelopes. This divergence of the amplitude A is a direct consequence of the degeneracy of system in Equation (20).

The caustic behavior can be present even in the trivial case of the free paraxial equation (with $V(x) = 0$) provided one begins with compressional initial data such as

$$u(x,0) = \partial_x S_{in}(x) = -\tanh(x). \tag{22}$$

In this $V(x) = 0$ case, the solution $\Psi^{(\hbar)}(x,t)$ of initial value problem equation (14a) can be represented exactly as a Fourier integral:

$$\Psi^{(\hbar)}(x,t) = \frac{1}{\sqrt{2\pi i\hbar t}} \int_{-\infty}^{+\infty} \times \exp\left(\frac{i}{\hbar}\left(\frac{(x-y)^2}{2t} + S_{in}(y)\right)\right) A_{in}(y)\, dy. \tag{23}$$

The behavior $\Psi^{(\hbar)}(x,t)$ as $\hbar \to 0$, uniformly in (x,t), can be obtained from an asymptotic (stationary phase) evaluation of this integral. The result shows that, away from the characteristic envelopes, $\Psi^{(\hbar)}(x,t)$ behaves asymptotically as the linear superposition

$$\Psi^{(\hbar)}(x,t) \sim \sum_j \exp\left(\frac{i}{\hbar} S^{(j)}(x,t)\right) A^{(j)}(x,t), \tag{24}$$

where the index j in the sum runs over different classical paths through the point (x,t), and $S^{(j)}$ is the classical path. $A^{(j)}$ is computed by integrating the transport equation along the jth classical path, with adjustments by phase shifts of the form $\exp(in^{(j)}\pi/4)$. The integers $n^{(j)}$ are computed from the number of times the jth path touches the caustic envelope.

In the linear case for general $V(x)$, the classical paths are not straight lines and the asymptotic behavior cannot be calculated with Fourier theory. Nevertheless, the asymptotic behavior is still given by the superposition of Eq. (24). Using the method of characteristics for the eikonal equation, one constructs a surface $u = u(x,t)$ over the (x,t) plane. With this surface, one integrates the transport equation for $A(x,t)$ and assembles the formula in Eq. (24). Arguments from the theory of uniform asymptotic expansions then show that the formula in Eq. (24) is asymptotically valid except at the focus and along the characteristic envelopes, the only effect of which is phase shifts of integer multiples of $\pi/4$.

In the linear case, the qualitative consequence of the formula in Eq. (24) is striking. Before the caustic, only one classical path passes through each space time point (x,t); only one term appears in the sum in Eq. (24); the intensity $|A(x,t)|^2$ is slowly varying on the $\hbar$ scale. After the caustic, three classical paths pass through each point (x,t), three terms appear in the sum, and the intensity $|A(x,t)|^2$ is

$$|A(x,t)|^2 = \left|\sum_j \exp\left(\frac{i}{\hbar} S^{(j)}(x,t)\right) A^j(x,t)\right|^2. \tag{25}$$

This has rapid oscillations on the $\hbar$ scale due to phase interference between the three terms in the sum. Mathematically, these rapid oscillations prevent strong convergence after the caustic. In summary, in this linear case the weak limit can be constructed simply by summing over the contributions from each classical path, with interference between terms in this sum causing rapid oscillations (Osman, 1998).

6. NONLINEAR SIMULATIONS OF DEFOCUSING AND FOCUSING CASES

Numerical results that illustrate the contrast formations of oscillations in solutions of Eq. (14a) (Osman, 1998) for the linear ($\gamma = 0$), the nonlinear defocusing ($\gamma > 0$), and the nonlinear focusing ($\gamma < 0$) cases are shown in this section. The linear case ($\gamma = 0$) is considered to illustrate the semiclassical linear theory just described. Figure 1 shows $|\Psi(x,t)|$ as a surface over the (x,t) plane, and clearly contains one focus of that theory, from which two caustics emanate.

Figure 2a shows that the defocusing case is treated here with a repulsive nonlinearity ($\gamma > 0$). As in the linear case, oscillation intensity forms at specific points in space and time, and then persists.

In the defocusing case, these oscillations form two packets, one travelling to the right and the other to the left. The central region of the spatial profile that separates the two oscillatory regions is a quiescent plateau at times beyond the focus. However, when compared with the linear case, several distinguishing features arise from the nonlinearity. First, the amplitude $|\Psi(x,t)|$ is much less intense at the focus than in the linear case, which is depicted from the same perspective in Figure 2b.

The response in the focusing case is treated here with an attractive nonlinearity ($\gamma < 0$; Fig. 3a). Indeed, the defocusing case had the mildest response, followed by the linear case, with the most extreme behavior found with focusing nonlinearity. It is the focusing nonlinearity that supports solitons in one spatial dimension and that blows up in finite time in two or more dimensions.

https://doi.org/10.1017/S0263034604221139 Published online by Cambridge University Press

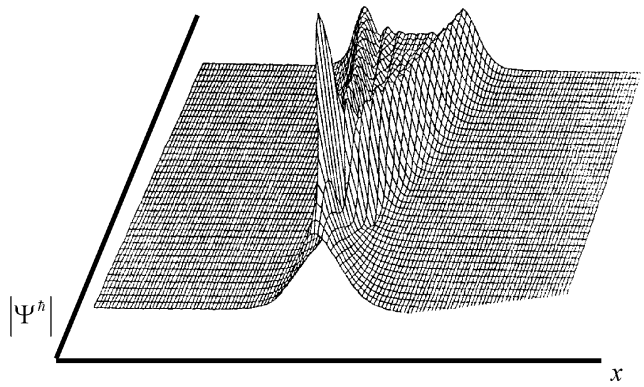

Fig. 1. The amplitude $|\Psi^{(\hbar)}|$ for the linear ($\gamma = 0$) paraxial equation as a surface over the (x, t) plane, for $\hbar = 0.1$.

The blowup of a portion of the oscillatory region shown in Figure 3b admits the intriguing interpretation of these oscillations as a dense "sea of solitons," located near the center of the spatial profile, with a sharp boundary separating the oscillatory from the quiescent regions of space.

7. CONCLUSION

In conclusion, this article investigated a numerical and theoretical study of the generation, and propagation, of oscillations in the semiclassical limit ($\hbar \to 0$) of the nonlinear paraxial equation at laser–plasma interaction. In a general setting of both dimension and nonlinearity, the essential differences between the focusing and defocusing cases were

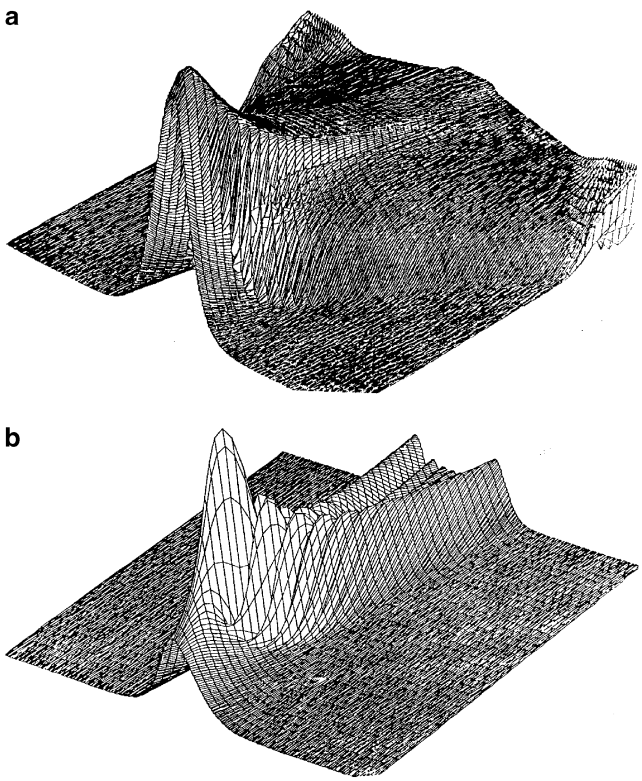

Fig. 2. a: The amplitude $|\Psi^{(\hbar)}|$ for the defocusing ($\gamma > 0$) nonlinear paraxial equation as a surface over the (x, t) plane, for $\hbar = 0.1$. b: The comparison result for the linear ($\gamma = 0$) paraxial equation.

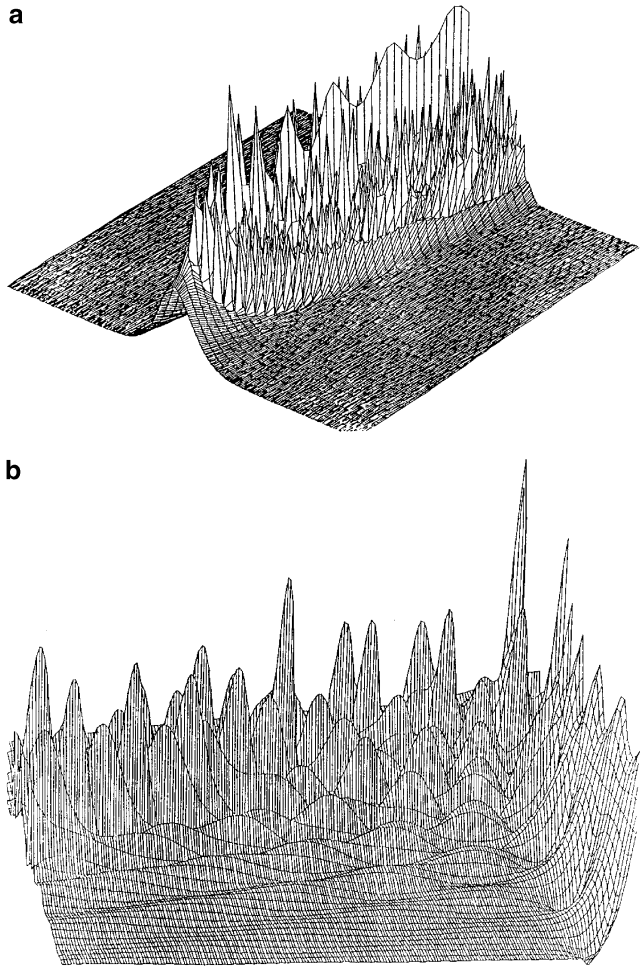

Fig. 3. a: The amplitude $|\Psi^{(\hbar)}|$ for the focusing ($\gamma < 0$) nonlinear paraxial equation as a surface over the (x, t) plane, for $\hbar = 0.1$. b: An enlargement of the oscillatory region from (a).

https://doi.org/10.1017/S0263034604221139 Published online by Cambridge University Press

investigated. Numerical comparisons of the oscillations are made between the solutions of the linear and nonlinear paraxial equation due to laser–plasma interactions.

This article has presented several numerical simulations that illustrate and contrast the formation of oscillations in solutions of Eq. (14a), for the linear ($\gamma = 0$), the nonlinear defocusing ($\gamma > 0$), and the nonlinear focusing ($\gamma < 0$) cases. In the first numerical simulation of Figure 1, the linear case of ($\gamma = 0$) was considered, to illustrate the semiclassical linear theory. Figure 1 illustrates $|\Psi(x,t)|$ as a surface over the (x,t) plane, and clearly contains one focus, from which two caustics emanate. Notice that $0(\hbar)$ wavelength oscillations in the intensity form at the focus and persist for later times. The spatial region containing these oscillations is bound by the two caustics.

Figure 2a treats the defocusing case with a repulsive nonlinearity ($\gamma > 0$). Figure 2a shows that, as in the linear case, oscillations in the intensity form at specific points in space and time, and then persist. However, when compared with the linear case, several distinguishing features arise from the nonlinearity. First, the amplitude $|\Psi(x,t)|$ is much less intense at the focus than in the linear case, which is depicted from the perspective, but with a different vertical scale shown in Figure 2b. Second, while the oscillations are given to be $0(1)$ in amplitude and $0(\hbar)$ in wavelength, this can be compared for the defocusing case. In the defocusing case, these oscillations form two packets, one travelling to the right and the other to the left. The central region of the spatial profile that separates the two oscillatory regions is a quiescent plateau at times beyond the focus.

Figure 3a treats the focusing case with an attractive nonlinearity ($\gamma < 0$). The response in this focusing case is the most violent of the three graphical forms presented. Indeed, the defocusing case had the mildest response, followed by the linear case, with the most extreme behavior found with focusing nonlinearity. It is the focusing nonlinearity that supports solitons in one spatial dimension and which blows up in finite time in two or more dimensions. The blowup of a portion of the oscillatory region illustrated in Figure 3b admits the intriguing interpretation of these oscillations as a dense "sea of solitons" space (Hora, 1991) located near the spatial profile, with a sharp boundary separating the oscillatory from the quiescent regions of space (Hora, 2000). This is discussed for application to the fast ignitor laser fusion scheme (Tabak *et al.*, 1993) especially for the condition avoiding the intermediary step of the funnel generation (Boreham *et al.*, 1998; Hora, 2000).

REFERENCES

Boreham, B., Bolton, P.R., Newman, D.S., Obolu, S., Hora, H., Aydin, M., Azechi, H., Cicchiellit, L., Eliezer, S., Goldsworthy, M.P., Häuser, T., Kasotakis, G., Kitagawa, Y., Martinez-Val, J.M., Mima, K., Murakami, M., Nishihara, K., Piera, M., Ray, P.S., Schied, W., Sarris, E., Stening, R.J., Takabe, H., Velarded, G., Yamanaka, M., Yamanaka, T., Castillo, R. & Osman, F. (1998). Beam matter interaction physics for fast ignitors. *Fusion Eng. Design.* **44**, 215.

Esarey, E., Sprangle, P., Kroll, N.M. & Ting, A. (1997). *IEEE J. Quantum Electron.* **QE-33**, 1879.

Fornberg, B. & Whitman, G.B. (1978). A numerical and theoretical study of certain nonlinear wave phenomena. *Phil. Trans. Roy. Soc. A* **289**, 373–404.

Häuser, T., Scheid, W. & Hora, H. (1992). *Phys. Rev. A* **45**, 1278.

Hora, H. (1991). *Plasmas at High Temperature & Density: Applications & Implications of Laser-Plasma Interaction.* Heidelberg, New York: Springer-Verlag.

Hora, H. (2000). *Laser Plasma Physics: Forces and the Nonlinearity Principle.* Bellingham, WA: SPIE Press.

Osman, F. (1998). Nonlinear Paraxial Equation at Laser Plasma Interaction. PhD Thesis, University of Western Sydney, Australia.

Tabak, M., Hammer, J., Glimsky, M.E., Kruer, W.L., Wilks, S.C., Woodworth, J., Campbell, E.M., Perry, M.D. & Mason, R.J. (1993). *Plasma Phys.* **1**, 1626.

Wang, J.X., Ho, Y.K., Kong, Q., Zhu, L.J., Feng, L., Scheid, W. & Hora, H. (1998). *Phys. Rev. E* **58**, 6575.

Zakharov, V.E. & Shabat, A.B. (1973). Exact theory of two-dimensional self-focusing and one-dimensional self-modulation of waves in nonlinear media. *Sov. Phys. JETP* **34**, 62–69.

https://doi.org/10.1017/S0263034604221139 Published online by Cambridge University Press